Chapter 10

Controlling the Biocompatibility and Mechanical Effects of Implantable Microelectrodes to Improve Chronic Neural Recordings in the Auditory Nervous System

Payton Lin, Yu Tsao and Li-Wei Kuo

Additional information is available at the end of the chapter

http://dx.doi.org/10.5772/intechopen.72659

Abstract

Implantable microelectrodes are useful for monitoring neural response patterns in the auditory cortex, however chronic neural recordings can often deteriorate with time (e.g. impedance measures across electrode arrays generally increase monotonically over the first 7 days post-implant). This problem is caused by the increasing spatial distribution of reactive tissue responses (corresponding to changes in impedance spectra along the electrode-tissue-interface). Therefore, the design of microelectrode probes must ensure that the neuronal ensembles lie within a cylindrical radius of the recording electrodes. In this chapter, chronic neural recording failure is examined via cortical spike patterns, histological analyses, indentation experiments, and finite element models. Next, the microfabrication of the "Utah" electrode array and the "Michigan" probe is compared to determine how their size, shape, and geometry address: (1) the spatial distribution of neurons (as related to recording quality); (2) the initial penetrating profile (as related to insertion killzones); (3) the reactive cell responses (as related to glial encapsulation); (4) the anchoring of the probe's position in the tissue (as related to micromotions) and (5) the embedding of various bioactive reagents (ex: growth factors, anti-inflammatory drugs, etc.). Finally, a novel hydrogel "Dropping Method" is proposed for controlling the biocompatibility and mechanical properties at the electrode-tissue-interface.

Keywords: auditory cortex, implantable microelectrode array, chronic neural recording, neural probe, brain machine interface, inflammatory response, biocompatibility, insertion killzone, glial encapsulation, micromotion, finite element model, hydrogel

1. Introduction

Brain machine interfaces connect the human brain to electronic devices and computer software [1]. Machine intelligence can offer the inherent advantages of greater processing speeds, computing power, memory capabilities, and even unrestricted sensory perception (e.g. infrared, ultra violet, X-ray, and ultrasonic spectra). With the emergence of deep brain stimulation, neuroprosthesis, neurofeedback, and exoskeleton technologies, science fiction is being bridged into a modern reality. However, the ultimate realization of a brain machine interface is to have a computer system that can chronically interface with the neural tissues. This neurotechnology will require neuroscientists and engineers to work together to address the technical challenges of accessing neural communication channels (for data routing and transmission), preserving the *biocompatibility* (to interface electronic components within the biological neural tissues), and maintaining the bio-signal processing (for selecting the appropriate control signals).

This chapter will focus on the *microelectrode*: a neural probe used in neurophysiology for either recording neural representations in the brain or for electrically stimulating the nervous tissue. Micromachined electrodes and microwires are often used to monitor the neuronal activities by characterizing extracellular field potentials of multiple active neurons. These neural interfaces are artificially-engineered extensions of the nervous system that must coexist in the precise connections of supporting glial cells, oligodendrocytes, astrocytes, and microglia (**Figure 1A**).

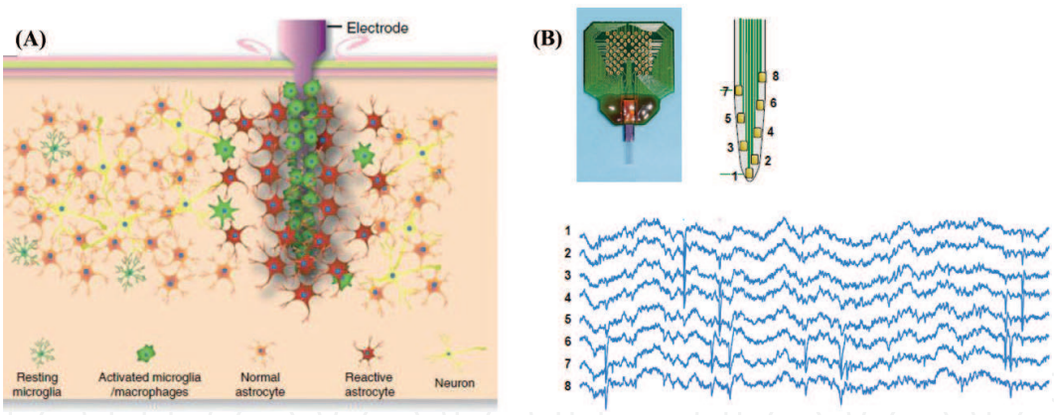

Figure 1. (A) Depiction of cellular changes induced by an implanted electrode and (B) multichannel neural recordings.

Multichannel microelectrodes (**Figure 1B**) can be used to monitor the activity in the *auditory cortex* and to investigate the functional organization of the auditory system [2–4]. For example, a chronic microelectrode investigation of the human auditory cortex [5] revealed a "tonotopic" pattern where the sound-driven units had excitatory receptive fields with sharply tuned best-frequency response over a range of frequencies. These micro-machined devices are currently being developed to control brain machine interfaces [6–8] and can benefit many applications in medicine, communication, entertainment, military, and education. However, there has been one limiting factor that has obstructed their reliability as a fully-implantable neural prosthesis: *chronic neural recordings* have been shown to deteriorate [9, 10] with time (**Figure 2**).

In Section 2, chronic neural recording failure is examined by reviewing cortical spike patterns, histological analyses, indentation experiments, and *finite element models* (FEM). For instance, probe impedance measures have been shown to increase, histological analyses have indicated that changes in the impedance spectra along the electrode-tissue interface are caused by the increasing spatial distribution of the reactive tissue responses, indentation experiments have shown persistent *inflammatory reactions* on the indwelling microelectrodes, and FEMs have simulated that surrounding tissues are compressed by the large stiffness mismatch of the implanted substrates (with pressure profiles revealing extensive tension at the probe tip).

In Section 3, the microfabrication of the *"Utah" electrode array* and the *"Michigan" neural probe* is compared by reviewing how their different sizes, shapes, and geometries can be redesigned to address: (1) the spatial distribution of neurons (as related to improving the recording quality); (2) the initial penetrating profile (as related to minimizing the *insertion killzone*); (3) the reactive cell responses (as related to preventing *glial encapsulation*); (4) the anchoring of a neural probe's position in the tissue (as related to reducing *electrode micromotion*) and (5) the embedding of various bioactive reagents (as related to eluting growth factors, anti-inflammatory drugs, etc.).

In Section 4, a *hydrogel coating* layer is proposed for improving the mechanical properties and *biocompatibility* at the electrode-tissue interface. Hydrogel coatings can be tailored to provide a buffer layer (for reducing stiffness mismatch), and to control the swelling properties to anchor the position of the probe in the tissue. In addition, a novel hydrogel coating method called the "*Dropping Method*" is proposed to control the mechanical properties at the electrode-tissue-interface. The Dropping Method will be compared versus the traditional "*Dipping Method*."

2. Chronic neural recording failure

2.1. Deterioration of neural recordings over time

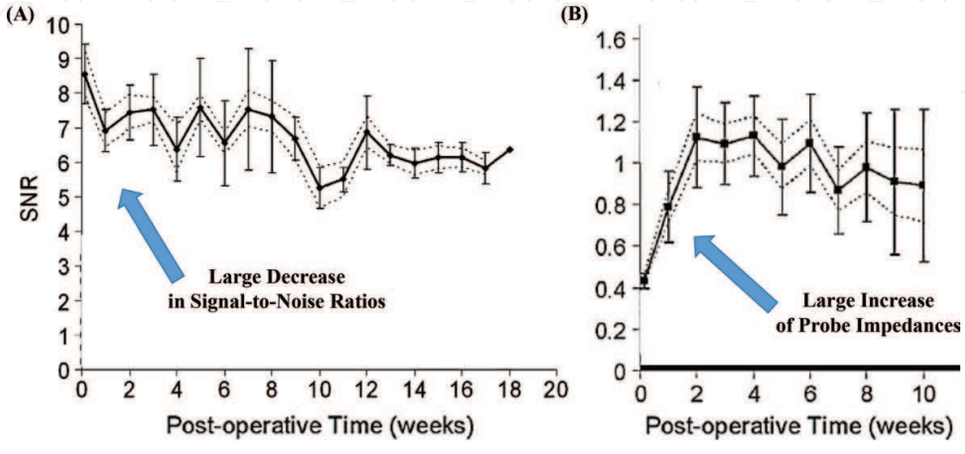

Figure 2. (A) Mean SNR across implanted probes over time and (B) mean impedance values. Reproduced from [10].

Silicon-substrate micromachined probes can provide high-quality multichannel spike activity recordings and local field potentials in the auditory cortex. For acute neural recordings, these measurements are generally stable. However, chronic long-term recordings are limited by the foreign body responses that occur during the wound healing process [9]. Previous research showed signal-to-noise-ratios (SNR) decreased as a function of postoperative time (**Figure 2A**) [10]. Impedance measures across electrode arrays were also shown to increase monotonically over the first 2 weeks (**Figure 2B**). This problem (of electrical signals gradually decreasing over time post-implant) must be solved to improve the chronic recording of neural activity.

Histological analyses have revealed tissue reactions to the implanted probe shanks during the assessment periods. For instance, confocal microscopy and immunohistochemistry protocols were used to measure the cellular density around the implanted electrodes and confirmed that a region of extensive reactive responses occurs around each individual electrode track [11]. By differentiating the spatial distribution of reactive tissue responses corresponding to changes in impedance spectra along the electrode-tissue interface, these findings confirm that reactive tissue responses directly influence the impedance spectra over time.

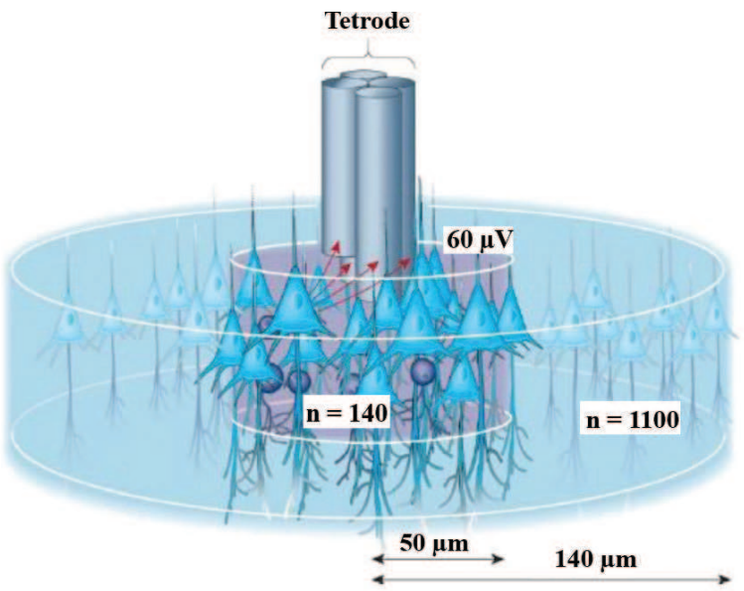

Figure 3. Unit isolation quality varies as a function of distance from the electrode. The spike amplitudes of the neuronal ensembles must lie within a cylindrical radius (n = 140 µm) to be detected. Reproduced from [12].

The recorded spike amplitudes were also measured as a function of the distance between the neuron and the electrode (by making comparisons from a multisite tetrode wire [12]). **Figure 3** shows that the extracellularly recorded spike amplitudes decreased rapidly with distance (a finding that indicates that the neuronal ensembles must lie within a cylindrical radius of ~140 µm of the recording electrode to effectively monitor the extracellular spike amplitudes). These *"cylindrical radius"* distances will be important to consider since previous studies have shown that the inflammatory responses can extend to ~100 µm.

http://dx.doi.org/10.5772/intechopen.72659

2.2. Insertion killzone

When inserting a microelectrode, the microshaft must penetrate through arteries, veins, tight junction cells, collagen, and smaller vessels in the pia. The shaft must then penetrate through tissues composed of neurons, glial cells, capillaries, arterioles, and venules. The tip of the shaft must be sharp enough to puncture through the microtubules and the fibrous structures within the neurofilaments. This electrode insertion process inevitably causes death and degeneration of its neighboring neurons and capillaries during the surgical implantation [13]. The *insertion killzone* is defined as the region around the shaft where the local neuron density is lower than the expected neuron density by a 90% confidence interval (**Figure 4A**). The tearing of neurons will cause the temporary loss of action potential capability and cell death due to the influx of calcium. The cutting of vessels and capillaries will cause microhemorrhages that can displace the neural tissue. If the neural tissue is compressed or stretched, the leakage of ions can lead to the loss of cellular homeostasis. Therefore, the penetrating shafts should be carefully fixed to a manipulator to prevent significant misalignment and to minimize the killzone (**Figure 4B**).

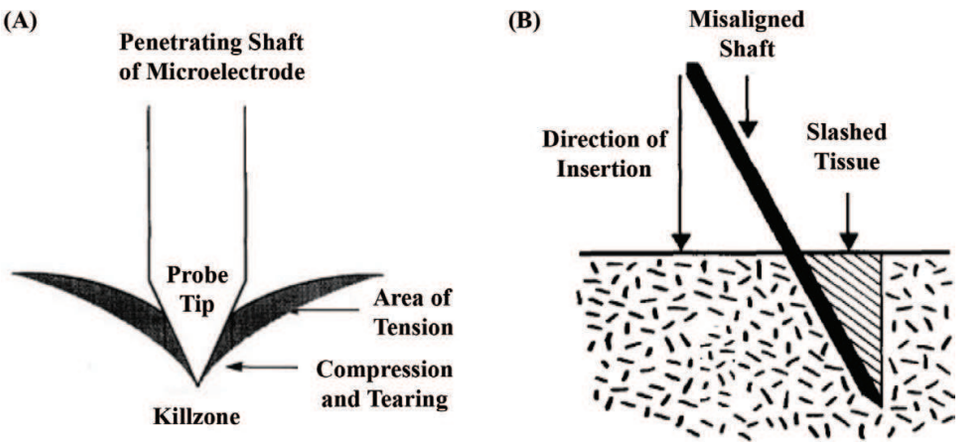

Figure 4. (A) Damage during insertion of a sharp microelectrode (where the shaft stretches the tissue beyond its elastic limits while passing through) and (B) significant axial misalignment of a shaft creates a swath of damage during insertion.

Penetrating shafts should be designed to minimize the initial mechanical trauma, to preserve the neuronal density in a local area around the implanted array, and to minimize the early reactive responses caused by the pathway of tissue damage. Indentation experiments have shown that immediate vascular and brain damage results in the recruitment of cells from the peripheral immune system and the activation of resident astrocytes or microglia. The reactive responses can be compared by immunochemically labelling for glial fibrillary acidic protein (GFAP), vimentin (for astrocytes), or ED1 (for microglia). When devices of different size were inserted, it was found that the volume of the reactive tissue responses was proportional to the cross-sectional area [14]. For instance, the smallest device (smallest cross-sectional area) with smooth surfaces and rounded corners caused less damage to the tissue, produced a smaller volume of reactive tissue, and left a smaller hole when removed from the tissue 1 week later.

2.3. Prolonged injury response

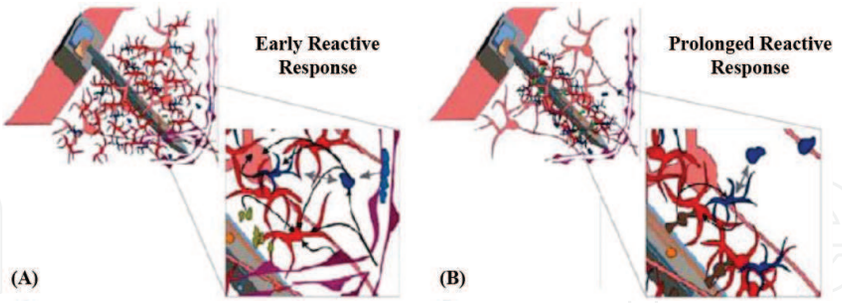

Figure 5. (A) Early reactive responses and (B) prolonged reactive responses to a chronically implant. Reproduced from [14].

An immunohistochemistry experiment [14] showed that the early reactive response (within 1 week (**Figure 5A**)) was associated with the amount of damage generated during the insertion (which depends on the device size or shape). However, this same study also showed that the prolonged reactive responses (after 4 weeks (**Figure 5B**)) eventually became similar (ultimately resulting in a compact cellular sheath containing astrocytes and microglia). While it is always better to minimize the insertion killzone, these results clearly indicate that a second sustained response occurs that is related to the tissue-device interactions. For instance, a long-term study [15] showed that the persistent ED1 up-regulation and neuronal loss (associated with the foreign body responses) were not observed in microelectrode stab controls (which indicates that the phenotype did not result from the initial mechanical trauma of the electrode implantation). Moreover, chronically-implanted electrodes were also covered in ED1/MAC-1 immunoreactive cells and released the pro-inflammatory cytokines MCP-1 and TNF-α (which are only characteristics of chronic inflammatory reactions). **Figure 6** shows that the zones of astrocytosis and connective tissue vary in proportion to an implant's reactivity [16]. Although the normal long-term response to an indwelling microelectrode is to develop a reactive glial tissue (that eventually forms into a fibrotic encapsulation layer or a glial scar), this sustained injury response has also been associated with chronic recording failure since the encapsulation (from persistent inflammatory reactions) isolates the electrodes from the surrounding neurons and decreases the stability and quality of the neural recordings.

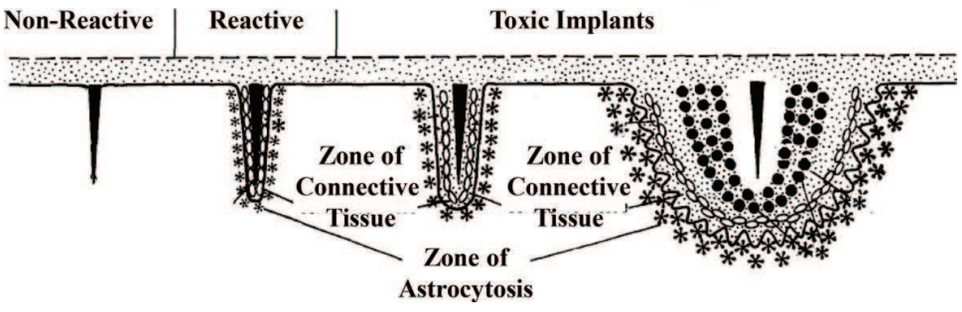

Figure 6. Histopathological changes that occur around a non-reactive implant, a reactive implant, and toxic implants.

http://dx.doi.org/10.5772/intechopen.72659

2.4. Micromotion

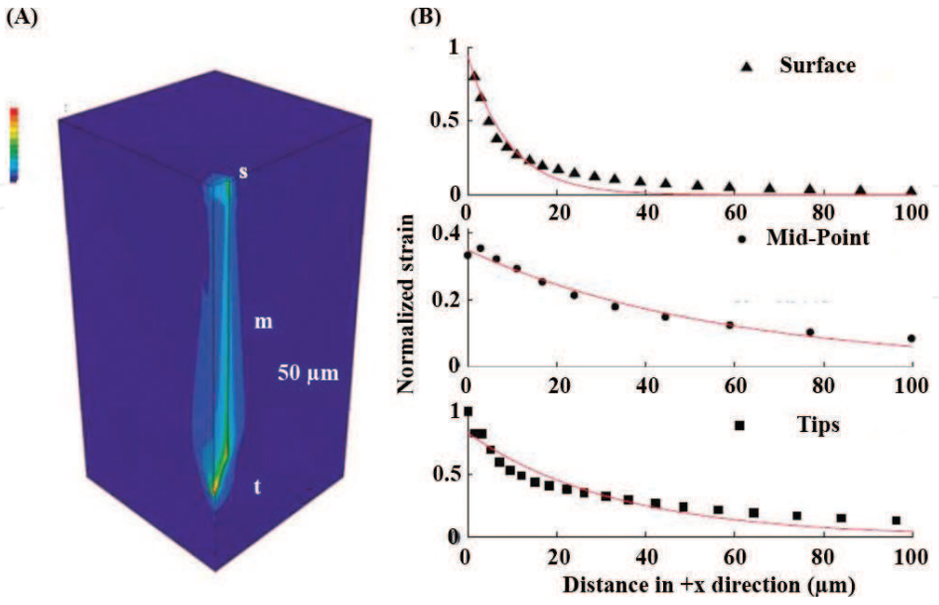

Figure 7. (A) Finite element model (FEM) strain profile of the radial tethering forces in the brain tissue that results from a 1 μm displacement of a silicon probe extended to 100 μm from the interface (s = surface, m = midpoint, t = tip). (B) Normalized strain values decreased exponentially as a function of distance in the brain tissue. Reproduced from [18].

The mechanical properties of the brain can be researched by mathematical simulation models that faithfully represent the geometry, material properties, and boundary or load conditions. For instance, an in-vivo indentation experiment [17] described the soft tissue deformation with a three-dimensional non-linear finite element model (FEM) of geometric information from the brain (obtained via magnetic resonance imaging techniques). Another FEM study measured the effects of tethering forces, probe-tissue adhesion, and the stiffness of the probe substrate on the interfacial strains induced around the implant site [18]. The results indicated that the interfacial strains were created by *micromotions* of the chronically implanted electrode, and that these mechanical strains around the implant site are likely responsible for the sustained tissue responses in chronic implants. In addition, the elevated strains at the probe tip were shown to cause poor probe-tissue adhesion and delamination of the tissue from the probe. The simulated probes also induced strain fields that displayed high radial tethering forces, with pressure profiles revealing extensive tension and maximum frictional shear stress at the tips of the arrays (**Figure 7**). Therefore, these findings indicate that softer substrates should be used to reduce the strain at the probe-tissue interface (to reduce tissue responses in chronic implants). Specifically, the magnitude of the micromotions should be reduced at the microelectrode's tip position to ensure the stability of the recordings at the cortical surface since gliosis is typically observed at the probe tips [13] (with up to a three-fold increase in the size of the surrounding glial sheath compared to at other areas of the arrays [19]). Micromotions and cortical surface displacements can also result from respiratory pulsations [20], behavioral sources [21], and the translational movements of the electrode's tethering lead wire [22] (which can occur due to the rotational acceleration of the head [23]).

3. Comparing "Utah" electrode arrays versus "Michigan" neural probes

Implantable probe designs have primarily focused on modifying the size, shape, or geometry to minimize reactive cell responses. For the *"Utah" electrode array* [24] and the *"Michigan" neural probe* [25], Section 3.1 compares the spatial distribution of neurons (as related to improving recording quality), Section 3.2 compares the initial penetrating profile (as related to minimizing the insertion kill-zone), Section 3.3 compares the reactive responses (as related to preventing glial encapsulation), Section 3.4 compares the anchoring of the probe's position in the tissue (as related to reducing electrode micromotion), Section 3.5 compares the embedding of bioactive reagents (as related to eluting growth factors, anti-inflammatory drugs, etc.).

3.1. Spatial distribution of neurons

3.1.1. Utah electrode array

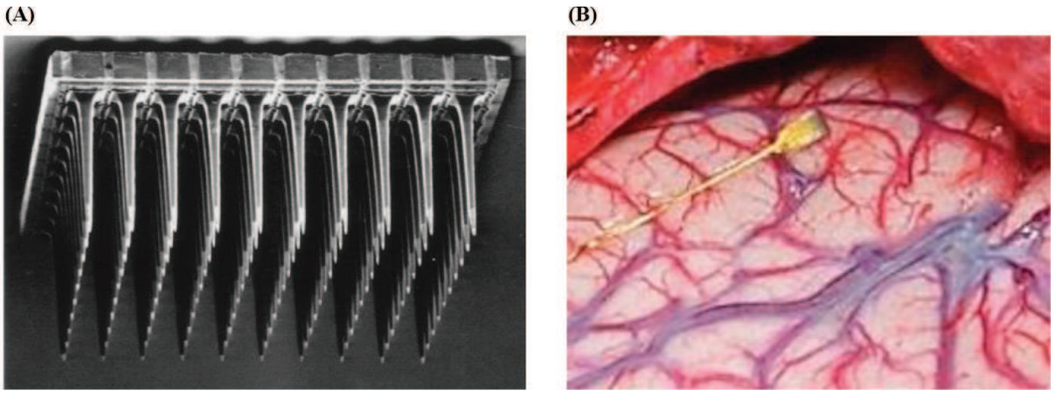

Figure 8. (A) The 100 microelectrode Utah electrode array and (B) the electrode probe tips implanted into the cortex.

The Utah array was designed from the ground up (with new manufacturing techniques [26]) to meet the specific needs of a multichannel neural interface [24]. Psychophysical experiments usually require evoking discriminable patterned percepts from many electrodes. Therefore, the Utah array (**Figure 8A**) was designed to possess a large number (~100) of large electrodes (~1.5 mm) that are typically in a square grid that projects out from a thin (~0.2 mm) substrate. **Figure 8B** shows the tapered electrodes suspended in a "sea of glass" substrate (that isolates each of the individual electrodes in the array from each other (~0.4 mm separation) to form a very effective dielectric insulating layer between the adjacent electrodes). The electrode probe tips are coated with platinum, gold, or iridium to facilitate the electronic to ionic transduction. The array's substrate was designed to be thick enough to prevent breaking upon insertion, but thin enough to rest on the cortical surface without producing a constant downward force on the array that could push it further into the cortex.

http://dx.doi.org/10.5772/intechopen.72659

3.1.2. Michigan neural probe

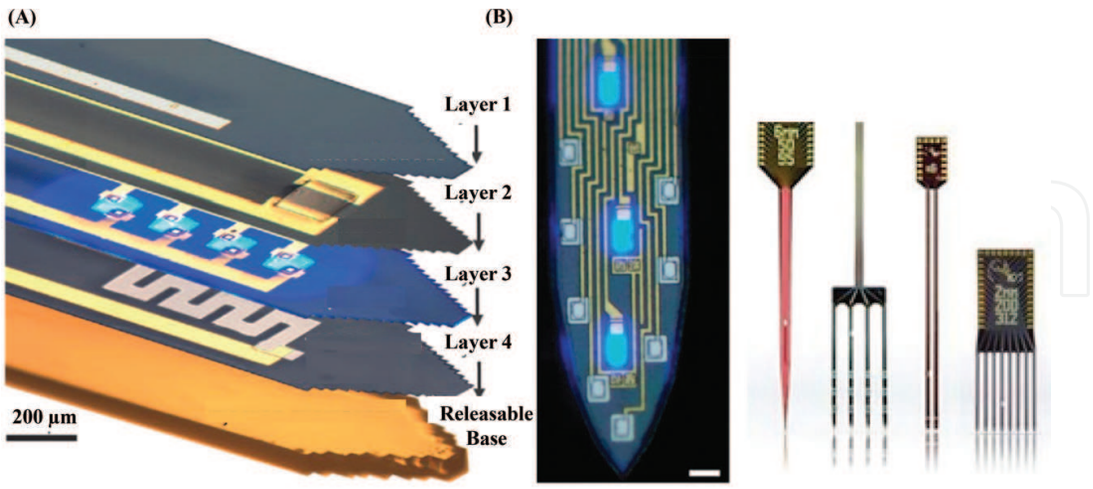

Figure 9. (A) Silicon-substrate Michigan probe and (B) microfabrication borrows semiconductors manufacturing methods.

Unlike the Utah electrode array [23], the planar Michigan probe [27] was only designed to take advantage of photolithographic manufacturing techniques from the semiconductor industry (**Figure 9A**). The extensibility of this platform technology enables these micromachined probes to be built with batch fabrication, easy customization of recording site placements or substrate shape, high reproducibility of geometrical/electrical characteristics, and the ability to integrate with ribbon cables or to incorporate on-chip electronics for signal conditioning (**Figure 9B**).

Unfortunately, the Michigan probes are known to induce a chronic breach of the blood–brain barrier [28] which leads to more chronic inflammation and culminates in neurodegeneration and ultimately to electrode failure (as described in Section 2). For instance, Michigan probes showed a significantly higher breach and worse wound-healing in comparison to microwires.

Since there is a trade-off between the size (spatial selectivity) and quality of signal recordings (sensitivity) in a neural microelectrode, previous research have altered the electrical properties by synthesizing biocompatible conducting polymers (**Figure 10A**) such as polypyrrole (PPy) and poly(3,4-ethylenedioxythiophene) (PEDOT) directly onto the electrode. Electrochemical deposition (**Figure 10B**) allows polymer films to be formed in a one-step process with a high degree of control over the film thickness and surface properties (e.g. with nanotubes in [27]).

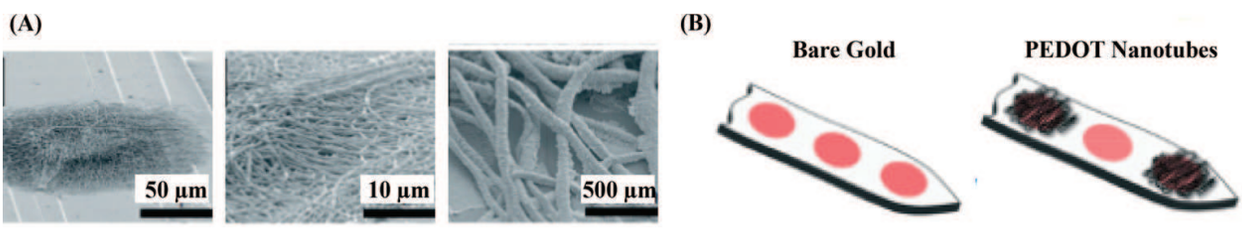

Figure 10. (A) Scanning electron microscope of deposited polymer and (B) uncoated vs. PEDOT nanotube (NT) electrodes.

3.2. Initial penetrating profile

3.2.1. Utah electrode array

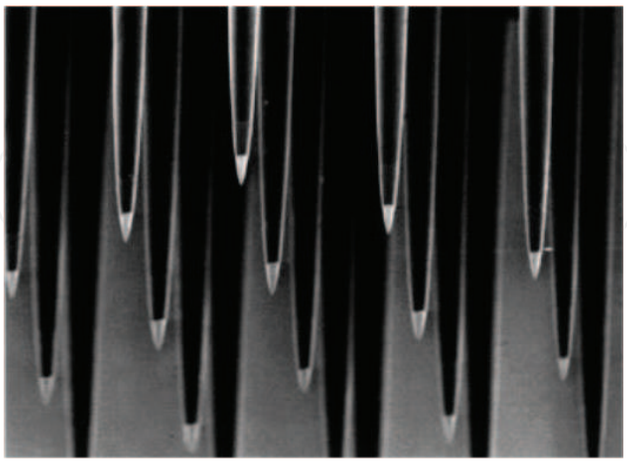

Figure 11. Penetrating shafts of the Utah electrode array with probe tips coated with platinum, gold, or iridium.

The penetrating electrodes of the Utah array (**Figure 11**) were designed to be slender enough to retain sufficient strength for withstanding the implantation procedure, yet to compromise as little cortical volume as possible (only 80 μm in diameter at the base). The needles were intentionally designed to have a cylindrical/conical geometry (rather than a planar geometry) to displace the tissues they are inserted (rather than cutting their way through). In addition, an "Impact Insertion" technique was designed to inject the array into the cortex at a high velocity [26]. This momentum transfer tool preserves uniformity and prevents dimpling of the cortex.

3.2.2. Michigan neural probe

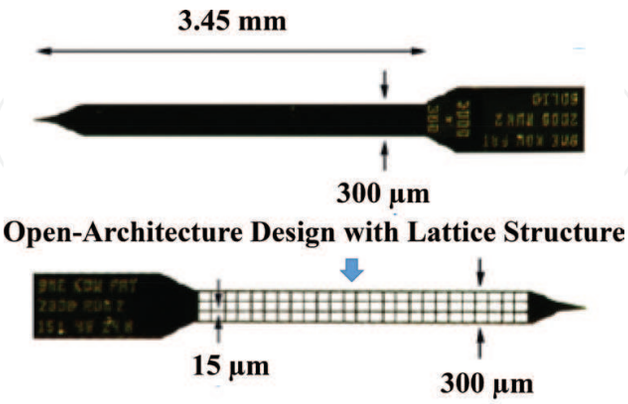

Figure 12. Comparison of a solid shank vs. the open-architecture design with a lattice structure. Reproduced from [25].

Despite evidence that smaller implants can increase the survival of neurons [29], the research direction for Michigan probes has been primarily guided by the *critical surface area model* [25]. This theory is supported by results showing microelectrodes with lattice structures (**Figure 12**)

exhibited less inflammation-related biomarker distribution in tissues compared to the solid shanks (even though both have identical penetrating profiles). However, Section 3.4.2 will show the alternative theory of *mechanical property differences* [30] can also explain these results.

3.3. Reactive processes

3.3.1. Utah electrode array

The electrodes are built from biocompatible materials such as silicon, silicon nitride, silicon dioxide, platinum, titanium, tungsten, and silicone. Histological analyses show the neuronal cell bodies remain in close apposition to the electrode tracks (especially in sections where the tracks are similar in diameter to blood vessels). The benign tissue response showed that a thin capsule (~2–5 microns) forms around each electrode track. Histological samples also revealed gliosis, fibrotic-tissue buildup between the array and the meninges, bleeding in some tracks, and some array displacement through the cortex. Despite these reactive responses, electrodes were shown to be able to record single- and multi-unit responses in the cortex for over 3 years (the longest intervals studied). Therefore, the stability of these units over periods of months provides the most compelling evidence for the biocompatibility [23].

3.3.2. Michigan neural probe

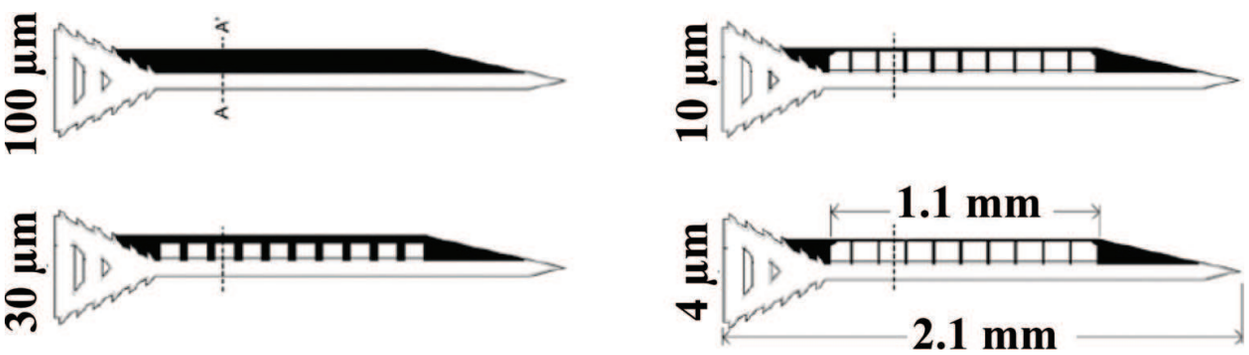

Figure 13. Comparison of a solid shank vs. open-architecture designs with varying lattice sizes. Reproduced from [30].

Glial sheaths (consisting of activated microglia and hypertrophied astrocytes, meningeal cells, and oligodendrocyte precursors that produce extracellular proteins that hinder local nerve regeneration) have been shown to form around the probe tract. As mentioned in Section 2, this tissue encapsulation is concomitant with a decrease in signal quality for neural recordings. Therefore, probe geometry has been investigated as a parameter for reducing chronic tissue encapsulation. Open-architectures (**Figure 13**) can reduce tissue encapsulation by presenting a narrow edge of surface area to prevent the prototypical attachment and spreading of foreign body responses (as cells would theoretically be unable to attach or create cytoskeleton tension below a certain dimension [30]). The tissue reactivity around the smallest lattice structure was expected to induce the least encapsulation. However, the comparison between probe designs indicated that the differences in encapsulation and neuronal loss was insignificant. Qualitative histology also showed similar responses inside the lattice region and around the shank. This has led to the *mechanical property differences* theory (which is discussed further in Section 3.4.2).

3.4. Anchoring of the probe's position

3.4.1. Utah electrode array

The large number of penetrating electrodes presents a very large surface area to the cortex and the implanted array tends to self-anchor to the cortical tissues. More importantly, the "sea of glass" allows the array to float in the cortical tissues as the cortex moves due to respiration, blood pumping, and skeletal displacements. This design feature produces an extremely stable interface with the surrounding neurons as it moves with the cortex and thereby produces very little micromotion between the electrode tips and the neurons near its active tips. In addition, GFAP staining showed that a fixation mode that un-tethers the implant from the skull elicits a smaller tissue reaction and results in the survival of a larger number of neurons in the region closest to the tissue interface [29].

3.4.2. Michigan neural probe

In Sections 3.2.2 and 3.3.2, the *critical surface model* was used to explain the benefits of open-architecture designs [25, 30]. However, an alternative theory [30] was offered to explain how the open-architecture designs reduce tissue encapsulations compared to the solid shanks. The theory of *mechanical property differences* assumes that lattice structures reduce the induced strain from relative movements (e.g. micromotion) between the probe and the tissue (occurring from the continual pulsations of vascular and respiratory oscillations). In other words, the adjoining lattice structure is assumed to present a more flexible mechanical interface that can improve the mechanical surface properties (relative to the solid probe shank). This competing theory of *mechanical property differences* is supported by FEM results that demonstrate that the shape of the electrode substantially influences the local pattern and the magnitude of strain around the electrode (especially at the electrode tip where the shank has a spear-head shape or at regions that have discontinuous or sharp edges [31]).

The theory of *mechanical property differences* is also supported by electrophysiological data [28] showing the Michigan electrode's recording performance failed faster relative to a microwire electrode. Since persistent micromotions are known to trigger a complex cascade of events, it was hypothesized that the different material properties and design of the Michigan electrode was the cause for the diminished wound healing response, the increased inflammation, the enhanced blood–brain barrier permeability, and the infiltration of inflammatory myeloid cells. For instance, a genomic analysis revealed an upregulation of MMP-2 (for facilitating wound healing and promoting neuronal regeneration) and blood–brain barrier stabilizing proteins in microwire electrodes (indicating enhanced stability and reduced micromotions compared to Michigan electrodes). Despite these findings, the *critical surface area model* theory is preferred over the theory of *mechanical property differences* because of previous results that have shown negligible differences in glial encapsulation between the soft and flexible parylene/SU-8-based structures in [30] and the silicon-based arrays (that are orders of magnitude stiffer) in [25].

http://dx.doi.org/10.5772/intechopen.72659

3.5. Embedding of bioactive reagents

3.5.1. Utah electrode array

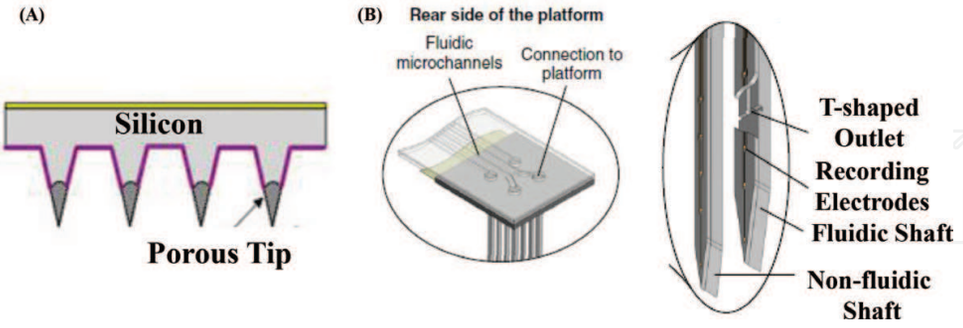

Figure 14. Platinum coated tips of the Utah electrode. Scale bar = 0.5 mm. Reproduced from [32, 33].

The microneedle array can be fabricated with porous tips that can be loaded with drugs that have a high molecular weight [32]. These porous tips are nano-structured silicon (**Figure 14A**), a material that is biocompatible, bioactive, biodegradable, and appropriate for the cultivation of adherent cells in-vivo without noticeable toxicity for biological applications. Drug delivery is also possible in the 3D floating silicon array by using a silicon platform that has microfluidic cables with adapters used for liquid supply [33]. Selected shafts can be equipped with fluidic integration (**Figure 14B**) with either one independent fluidic channel (to maximize the volume coverage) or two independent microchannels (to infuse both a drug and a buffer reference at the same location) when combining drug delivery within the array of recording electrodes.

3.5.2. Michigan neural probe

Planar microelectrodes can directly utilize innovations from micro-fabrication technology and lab-on-a-chip delivery devices. For instance, aerosol jet printing technology can be utilized to directly construct a patterned neural interface with anti-inflammatory nanocarriers [34]. 3D probe structures with microfluidic channels can also be fabricated via surface micromachining and deep reactive ion etching (DRIE) [35]. Neural probe designs (**Figure 15**) can also be bulk-microfabricated to include microchannels along the shanks for microscale and controlled fluid delivery through the blood–brain barrier [36].

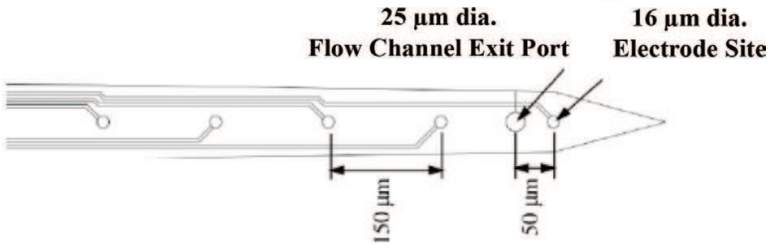

Figure 15. Probe design with microchannels along the shanks for controlled fluid delivery. Reproduced from [36].

4. Hydrogel improves biocompatibility and mechanical properties

4.1. Improved biocompatibility

Hydrogels such as Alginate are naturally occurring polysaccharides that are typically obtained from brown algae seaweed (**Figure 16**). These water-soluble biomaterials have many versatile properties such as gelling and film-forming. Hydrogels are biocompatible and are commonly used in biomedical or tissue engineering applications. Hydrogels are formed by cross-linking hydrophilic organic components and can respond to specific environmental changes [37]. This makes hydrogels the ideal polymer matrix for controlling the delivery of drugs and bioactive components into a complex biologic system.

Alginate hydrogels have been successfully applied as a coating on the Michigan probes. One study [38] showed that biodegradable neurotrophin-eluting hydrogels can be applied on the microelectrode arrays to attract neurites to the surface of the electrodes (for improved neuron-electrode proximity). Hydrogels can also be loaded with nanoparticles of anti-inflammatory agent dexamethasone (DEX) for drug delivery [39]. In-vitro drug release kinetics has revealed that 90% of the DEX can be successfully released from entrapped nanoparticles over 2 weeks. In addition, the impedance of the nanoparticle-loaded hydrogel coatings on microfabricated neural probes were equivalent to the unmodified/uncoated probes controls (indicating that the loaded-nanoparticles do not hinder electrical transport). Most importantly, the chronically implanted electrodes loaded with DEX were shown to maintain impedances in-vivo (unlike the control electrodes that showed increases after 2 weeks of implantation). This improvement in chronic neural recordings indicates the DEX-modified neural probes reduced the amount of glial inflammation via local administration of therapeutic agents. Hydrogels can also be used as a scaffold to encapsulate drug-incorporated biodegradable nanofibers for a more sustained and slower release (to reduce the burst effect [40]).

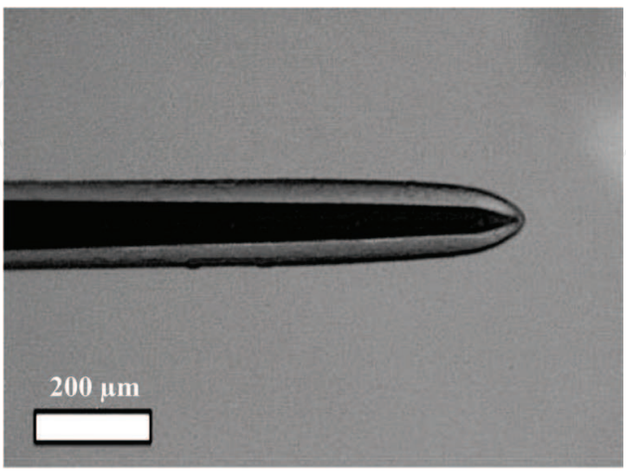

Figure 16. Optical microscopy image of an Alginate hydrogel coating on a Michigan probe. Reproduced from [41].

4.2. Improved mechanical properties

Hydrogels have also been proposed to improve the mechanical properties of the implantable microelectrodes. First, hydrogel coatings can be dehydrated to minimize the initial penetrating profile [41]. Second, the degree of reswelling can be controlled by using different cross-linking molecules to better anchor the position of the probe in the tissue after the implantation [42]. Third, the shear moduli of a hydrogel can be tightly regulated by controlling the cross-linking densities to reduce the stiffness mismatch between the hard silicon-based probes (~100 GPa) and the soft tissue (~10 kPa). Fourth, the uniformity of the hydrogel coating can be controlled by changing the concentration of the solution. Lastly, the hydrogel thickness can be controlled by quickly drying the coated surfaces in air and then overlaying additional layers on top.

Despite the many advantages of hydrogels, the spatial distribution of neurons (as it relates to recording quality) has been a barrier to the practical implementation of hydrogel coatings on microelectrodes. For instance, neural recordings in the auditory cortex showed a significant loss in functionality (as determined by the number of clearly detectable units and the average signal-to-noise ratios [43]). In fact, in-vivo experiments showed that only 30% of the electrode sites (with 80 μm thick hydrogel coatings) could record detectable signals from surrounding neurons and that the average signal-to-noise ratio dramatically decreased (even for 5 μm thick coatings). The loss in neural recording quality is hypothesized to be caused by the reswelling properties of the dehydrated hydrogel coatings (which can affect the spatial distribution of the target neurons around the implanted electrode). In other words, the low signal detection is hypothesized to be caused by the post-implantation water absorption which pushes the target neurons away from the electrode surfaces as they rehydrate (and beyond the *cylindrical radius* distances in [12] that are required for effective electrode recording, as illustrated in **Figure 3**).

To solve the hydrogel swelling problem, [44] proposed to modify the electrode design to place the recording sites in closer proximity to the hydrogel's surface (**Figure 17**). The deposition of conducting polymer PEDOT has also been shown to restore some of the lost functionality of electrode sites with thicker hydrogel coatings [43]. Alternatively, fibrin can be selected (rather than Alginate) to be reabsorbed in the surrounding tissues 7 days after the implantation [45].

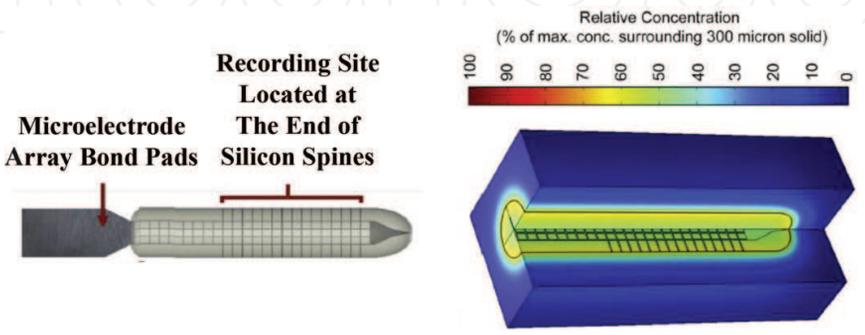

Figure 17. Electrode design with recording sites in closer proximity to the hydrogel's surface. Reproduced from [44].

4.3. The "Dipping Method"

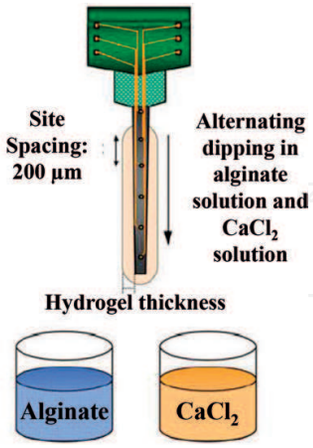

Figure 18. Dipping Method for hydrogel coating of neural electrodes with optical microscopy. Reproduced from [43].

While previous solutions to the hydrogel swelling problem have mostly proposed physical changes to the actual microelectrode or the hydrogel [39–45], most attempts still rely on the "*Dipping Method*" for depositing the hydrogel coatings onto the microelectrodes (as proposed in [41]). **Figure 18** shows the Dipping Method involves the repetitive dipping of electrodes (e.g. via an inverted fine-tooth syringe pump [44]) into an alginate solution followed by immersion in a $CaCl_2$ solution until a desired coating thickness is achieved. The thickness of the hydrogel coating is roughly controlled by monitoring the sample as a function of the number of dips with an optical microscope [43]. For instance, 1 dip is sufficient for a thin coating, and roughly 20 dips are needed to obtain a thick diameter coating. The hydrogel-coated electrodes are then dried in a laminar hood [43] or by exchanging ethanol and drying in an air stream [40].

In practice, the Dipping Method has several problems. First, lateral movements of the neural electrode effect the reproducibility of the alginate coating around the shank of the probe [40]. Second, it is impossible to control the average thickness by just approximating the number of dipping cycles (as verified by ellipsometry data in Figure 4B of [44]). Third, it is impossible to control the maximum radial thickness by just altering the number of dips (as demonstrated in Figure 2C of [45]). Fourth, the speed of dipping effects the uniformity of the alginate coating around the shank of the probe [40]. These limitations of the Dipping Method are confounding and counter-productive when considering that the entire rationale for using hydrogel coatings was to control the mechanical properties of the electrodes in [41]. Furthermore, the Dipping Method requires a human observer to subjectively monitor the entire dipping process with an optical microscope [43]. Therefore, this proposed Dipping Method essentially eliminates one of the primary advantage of the Michigan probes: exploiting semiconductor manufacturing techniques to allow batch fabrication for the high reproducibility of geometrical/electrical characteristics (as highlighted in Section 3.1.2).

http://dx.doi.org/10.5772/intechopen.72659

4.4. The "Dropping Method"

Techniques for coating hydrogels onto microelectrodes include spray coating, brush coating, Dipping Methods [39–45], and micropipetting [38]. Unfortunately, none of these methods can produce uniform coatings in a reproducible manner [46]. Therefore, novel strategies such as the Molding Method (which involves the photopolymerization of hydrogels in a polyethylene tube) have been proposed to provide hydrogel coatings that are more reproducible and have a means to control coating uniformity and thickness (e.g. by varying the polyethylene tubing).

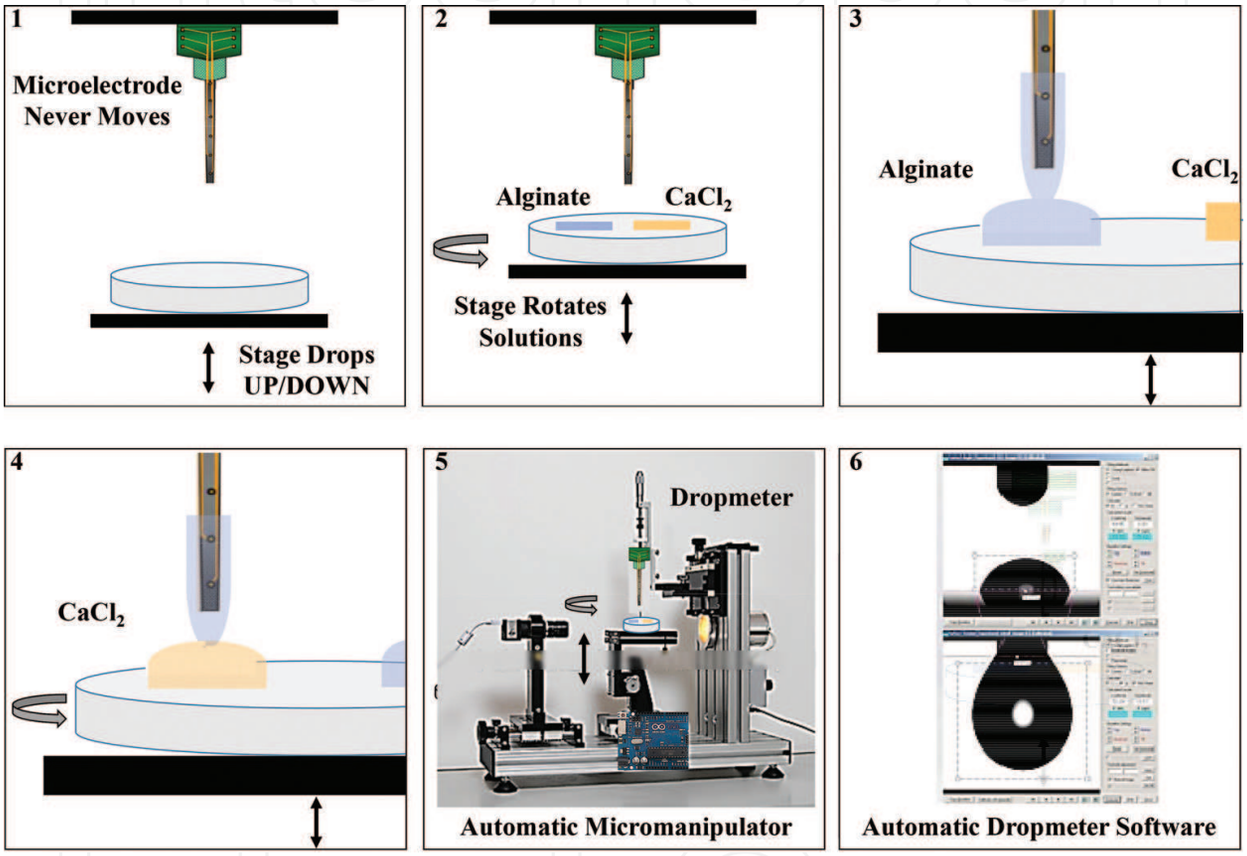

Figure 19. Dropping Method for hydrogel coating of neural electrodes with a fully-automated procedure.

Figure 19 proposes a novel procedure called the "Dropping Method" to address the reported limitations of the Dipping Method. First, the microelectrode is permanently attached in one location to eliminate lateral movements (to improve reproducibility [40]). Second, a stage that contains solutions is automatically revolved to eliminate the requirement of approximating movements (to improve the average thickness [44]). Third, the stage is dropped downward to allow gravity to align the droplets and to evenly pull down the edges (to improve the radial thickness [45]). Fourth, the speed of dropping is automated by a digital micromanipulator (to improve the uniformity of the alginate coating around the shank of the probe [40]). Finally, the optimal contact angle is automated on a Dropmeter stage via programmable software (instead of relying on subjective interpretations of a human observer via optical microscopy as in [43]).

FEM and histological analyses have shown that elevated local strains correspond to increases in gliosis (with a three-fold increase in gliosis at the probe tips compared to other areas of the explanted arrays [19]). In addition, FEM pressure profiles predict that the strain at the tip can be reduced by utilizing more flexible or softer substrates, reducing the opening angle of the probe face, and by promoting tissue integration to reduce excessive adhesion. Therefore, the Dropping Method is recommended for coating hydrogel at the tips of the microelectrodes to optimize the mechanical effects for improved chronic recording stability. Applying hydrogel coatings on the probe tips should stabilize the mechanical interface and lower the interfacial tension with the surrounding biological environment. Constraining hydrogel coating depths to just the tips will also avoid the electrode coverage issue [12]. Finally, the initial penetrating profile should be reduced since only the dehydrated probe tips will reswell in thickness upon water absorption (unlike previous studies that coated the hydrogel layers along the entire length of the neural electrode shanks in efforts to reduce the sustained injury responses).

5. Conclusions

This chapter reviewed how controlling the biocompatibility and mechanical properties of a microelectrode is critical when implanting deeper within the auditory system. To effectively monitor extracellular spike amplitudes in the cortex, several design considerations should be factored to ensure that the neuronal ensembles lie within a cylindrical radius of the recording electrode. First, penetrating shafts should reduce the initial mechanical trauma during surgical implantation (to minimize the reactive responses caused by the pathway of tissue damage). Second, the indwelling microelectrodes should embed bioactive reagents since chronic neural recording failure is associated with sustained injury responses from persistent inflammatory reactions. Third, the mechanical properties should be controlled since micromotions can cause shearing and compression to the surrounding tissues (due to the large stiffness mismatch of the implanted substrates). This chapter also describes how hydrogels can minimize the cross-sectional area while ensuring the neuronal density is maintained in local areas surrounding the implant. A novel hydrogel coating "Dropping Method" is proposed instead of the Dipping Method to eliminate the problems of lateral movements, approximated cycles, and uniformity.

Acknowledgements

In this chapter, some parts of this work was performed when the first author was with the Centre for Biosystems, Neuroscience, and Nanotechnology, City University of Hong Kong, Hong Kong, with Stella Pang. The author is now working at the Center for Information Technology Innovation (CITI), Academia Sinica, Taipei, Taiwan with Yu Tsao.

http://dx.doi.org/10.5772/intechopen.72659

Glossary

Auditory cortex: region of the temporal lobe that is responsible for processing auditory information.

Biocompatibility: ability of a biomaterial to perform with an appropriate host response in the body.

Brain machine interface: technology that allows direct communication pathways between the brain.

Chronic neural recordings: long-term neural recordings by implantable (e.g. intracortical) electrodes.

Critical surface area model: theory of minimizing electrode surfaces to reduce tissue encapsulations.

Cylindrical radius: neuronal ensembles must lie within ~140 μm of the recording electrode [12].

Dipping method: hydrogel coating as a function of the number of dips (via optical microscopy).

Dropping Method: hydrogel coating automated on Dropmeter stage (via programmable software).

Electrode micromotion: induced strain from relative movements between the probe and the tissue.

Finite element model: numerical analysis that can approximate the behavior of mechanical systems.

Glial encapsulation: formation of a fibrotic encapsulation layer or a glial scar surrounding an implant.

Hydrogel coating: biomaterials with many versatile properties such as gelling and film-forming.

Inflammatory reactions: complex biological responses of tissues that protect from harmful stimuli.

Insertion killzone: region around the shaft where the local neuron density is lower than expected.

Utah electrode array: 3D arrays consisting of conductive needles (designed at University of Utah).

Mechanical property difference: theory of minimizing micromotions to reduce tissue encapsulation.

Michigan probe: planar shanks from semiconductor platforms (designed at University of Michigan).

Microelectrode: electrical conductor used for recording neural representations in the brain.

Author details

Payton Lin[1,2]*, Yu Tsao[2] and Li-Wei Kuo[3]

*Address all correspondence to: paytonlin20@gmail.com

1 Centre for Biosystems, Neuroscience, and Nanotechnology (CBNN), City University of Hong Kong, Hong Kong SAR

2 Academia Sinica, Center for Information Technology Innovation, Taipei, Taiwan

3 National Health Research Institute, Institute of Biomedical Engineering and Nanomedicine, Taiwan

References

[1] Kennedy PR, Bakay RAE, Moore MM, Adams K, Goldwaith J. Direct control of a computer from the human nervous system. IEEE Transactions on Rehabilitation Engineering. 2000;**8**:198-202

[2] Merzenich MM, Brugge JF. Representation of the cochlear partition on the superior temporal plane of the macaque monkey. Brain Research. 1973;**50**(2):275-296

[3] Rauschecker JP, Tian B, Hauser M. Processing of complex sounds in the macaque nonprimary auditory cortex. Science. 1995;**268**:111-114

[4] Kaas JH, Hacket TA. Subdivisions of auditory cortex and processing streams in primates. Proceedings of the National Academy of Sciences. 2000;**97**(22):11793-11799

[5] Howard MA, Volkov IO, Abbas PJ, Damasio H, Ollendieck MC, Granner MA. A chronic microelectrode investigation of the tonotopic organization of the human auditory cortex. Brain Research. 1996;**724**(2):260-264

[6] Sanchez JC, Principe JC, Nishida T, Bashirullah R, Harris JG, Fortes JA. Technology and signal processing for brain-machine interfaces. IEEE Signal Processing Magazine. 2008; **25**(1):29-40

[7] Moxon KA, Kalkhoran NM, Markert M, Sambito MA, McKenzie JL, Webster JT. Nanostructured surface modification of ceramic-based microelectrodes to enhance biocompatibility for a direct brain-machine interface. IEEE Transactions on Biomedical Engineering. 2004;**51**(6):881-889

[8] Polikov VS, Tresco PA, Reichert WM. Response of brain tissue to chronically implanted neural electrodes. Journal of Neuroscience Methods. 2005;**148**(1):1-18

[9] Kim GB, Fattahi P, Abidian MR. Electrode–neural tissue interactions: Immune responses, current technologies, and future directions. In: Taubert A, Mano JF, Rodríguez-Cabello JC, editors. Biomaterials Surface Science. Weinheim, Germany: Wiley-VCH Verlag GmbH & Co. KGaA; 2013. p. 539-565

[10] Vetter RJ, Williams JC, Hetke JF, Nunamaker EA, Kipke DR. Chronic neural recording using silicon-substrate microelectrode arrays implanted in cerebral cortex. IEEE Transactions on Biomedical Engineering. 2004;**51**(6):896-904

[11] Williams JC, Hippensteel JA, Dilgen J, Shain W, Kipke DR. Complex impedance spectroscopy for monitoring tissue responses to inserted neural implants. Journal of Neural Engineering. 2007;**4**(4):410

[12] Buzsáki G. Large-scale recording of neuronal ensembles. Nature Neuroscience. 2004;**7**(5): 446

[13] Edell DJ, Toi VV, Mcneil VM, Clark LD. Factors influencing the biocompatibility of insertable silicon microshafts in cerebral cortex. IEEE Transactions on Biomedical Engineering. 1992;**39**(6):635-643

[14] Szarowski DH, Andersen MD, Retterer S, Spence AJ, Isaacson M, Craighead HG, Turner JN, Shain W. Brain responses to micro-machined silicon devices. Brain Research. 2003;**983**(1):23-35

[15] Biran R, Martin DC, Tresco PA. Neuronal cell loss accompanies the brain tissue response to chronically implanted silicon microelectrode arrays. Experimental Neurology. 2005;**195**(1): 115-126

[16] Stensaas SS, Stensaas LJ. Histopathological evaluation of materials implanted in the cerebral cortex. Acta Neuropathologica. 1978;**41**(2):145-155

[17] Miller K, Chinzei K, Orssengo G, Bednarz P. Mechanical properties of brain tissue in-vivo: Experiment and computer simulation. Journal of Biomechanics. 2000;**33**(11):1369-1376

[18] Subbaroyan J, Martin DC, Kipke DR. A finite-element model of the mechanical effects of implantable microelectrodes in the cerebral cortex. Journal of Neural Engineering. 2005;**2**(4):103

[19] Hoogerwerf AC, Wise KD. A three-dimensional microelectrode array for chronic neural recording. IEEE Transactions on Biomedical Engineering. 1994;**41**(12):1136-1146

[20] Britt RH, Rossi GT. Quantitative analysis of methods for reducing physiological brain pulsations. Journal of Neuroscience Methods. 1982;**6**(3):219-229

[21] Fee MS. Active stabilization of electrodes for intracellular recording in awake behaving animals. Neuron. 2000;**27**(3):461-468

[22] Gilletti A, Muthuswamy J. Brain micromotion around implants in the rodent somatosensory cortex. Journal of Neural Engineering. 2006;**3**(3):189

[23] Goldstein SR, Salcman M. Mechanical factors in the design of chronic recording intracortical microelectrodes. IEEE Transactions on Biomedical Engineering. 1973;**4**:260-269

[24] Normann RA, Maynard EM, Rousche PJ, Warren DJ. A neural interface for a cortical vision prosthesis. Vision Research. 1999;**39**(15):2577-2587

[25] Skousen JL, Merriam SM, Srivannavit O, Perlin G, Wise KD, Tresco PA. Reducing surface area while maintaining implant penetrating profile lowers the brain foreign body response to chronically implanted planar silicon microelectrode arrays. Progress in Brain Reserach. 2011;**194**:167-180

[26] Jones KE, Campbell PK, Normann RA. A glass/silicon composite intracortical electrode array. Annals of Biomedical Engineering. 1992;**20**(4):423-437

[27] Seymour JP, Wu F, Wise KD, Yoon E. State-of-the-art MEMS and microsystem tools for brain research. Microsystems & Nanoengineering. 2017;**3**:16066

[28] Saxena T, Karumbaiah L, Gaupp EA, Patkar R, Patil K, Betancur M, Garrett B, Bellamkonda RV. The impact of chronic blood–brain barrier breach on intracortical electrode function. Biomaterials. 2013;**34**(20):4703-4713

[29] Thelin J, Jörntell H, Psouni E, Garwicz M, Schouenborg J, Danielsen N, Linsmeier CE. Implant size and fixation mode strongly influence tissue reactions in the CNS. PLoS One. 2011;**6**(1):e16267

[30] Seymour JP, Kipke DR. Neural probe design for reduced tissue encapsulation in CNS. Biomaterials. 2007;**28**(25):3594-3607

[31] Lee H, Bellamkonda RV, Sun W, Levenston ME. Biomechanical analysis of silicon microelectrode-induced strain in the brain. Journal of Neural Engineering. 2005;**2**(4):81

[32] Ji J, Tay FE, Miao J, Iliescu C. Microfabricated microneedle with porous tip for drug delivery. Journal of Micromechanics and Microengineering. 2006;**16**(5):958

[33] Spieth S, Brett O, Seidl K, Aarts AAA, Erismis MA, Herwik S, Trenkle F, Tatzner S, Auber J, Daub M, Neves HP, Puers R, Paul O, Ruthner P, Zengerle R. A floating 3D silicon microprobe array for neural drug delivery compatible with electrical recording. Journal of Micromechanics and Microengineering. 2011;**21**(12):125001

[34] Huang WC, Lai HY, Kuo LW, Liao CH, Chang PH, Liu TC, Chen SY, Chen YY. Multifunctional 3D patternable drug-embedded nanocarrier-based interfaces to enhance signal recording and reduce neuron degeneration in neural implantation. Advanced Materials. 2015;**27**(28):4186-4193

[35] Retterer ST, Smith KL, Bjornsson CS, Neeves KB, Spence AJ, Turner JN, Shain W, Isaacson MS. Model neural prostheses with integrated microfluidics: A potential intervention strategy for controlling reactive cell and tissue responses. IEEE Transactions on Biomedical Engineering. 2004;**51**(11):2063-2073

[36] Rathnasingham R, Kipke DR, Bledsoe SC, McLaren JD. Characterization of implantable microfabricated fluid delivery devices. IEEE Transactions on Biomedical Engineering. 2004;**51**(1):138-145

[37] Gong C, Wong KL, Lam MH. Photoresponsive molecularly imprinted hydrogels for the photoregulated release and uptake of pharmaceuticals in the aqueous media. Chemistry of Materials. 2008;**20**(4):1353-1358

[38] Winter JO, Cogan SF, Rizzo JF. Neurotrophin-eluting hydrogel coatings for neural stimulating electrodes. Journal of Biomedical Materials Research Part B: Applied Biomaterials. 2007;**81**(2):551-563

[39] Kim DH, Martin DC. Sustained release of dexamethasone from hydrophilic matrices using PLGA nanoparticles for neural drug delivery. Biomaterials. 2006;**27**(15):3031-3037

[40] Abidian MR, Martin DC. Multifunctional nanobiomaterials for neural interfaces. Advanced Functional Materials. 2009;**19**(4):573-585

[41] Kim DH, Abidian M, Martin DC. Conducting polymers grown in hydrogel scaffolds coated on neural prosthetic devices. Journal of Biomedical Materials Research Part A. 2004;**71**(4):577-585

[42] Lee KY, Rowley JA, Eiselt P, Moy EM, Bouhadir KH, Mooney DJ. Controlling mechanical and swelling properties of alginate hydrogels independently by cross-linker type and cross-linking density. Macromolecules. 2000;**33**(11):4291-4294

[43] Kim DH, Wiler JA, Anderson DJ, Kipke DR, Martin DC. Conducting polymers on hydrogel-coated neural electrode provide sensitive neural recordings in auditory cortex. Acta Biomaterialia. 2010;**6**(1):57-62

[44] Skousen JL, Bridge MJ, Tresco PA. A strategy to passively reduce neuroinflammation surrounding devices implanted chronically in brain tissue by manipulating device surface permeability. Biomaterials. 2015;**36**:33-43

[45] De Faveri S, Maggiolini E, Miele E, De Angelis F, Cesca F, Benfenati F, Fadiga L. Bio-inspired hybrid microelectrodes: A hybrid solution to improve long-term performance of chronic intracortical implants. Frontiers in Neuroengineering. 2014;**7**(7):1-12

[46] Jhaveri SJ, Hynd MR, Dowell-Mesfin N, Turner JN, Shain W, Ober CK. Release of nerve growth factor from HEMA hydrogel-coated substrates and its effect on the differentiation of neural cells. Biomacromolecules. 2008;**10**(1):174-183

IntechOpen